

SYMPLECTIC FINITE DIFFERENCE APPROXIMATIONS OF THE NONLINEAR KLEIN–GORDON EQUATION*

D. B. DUNCAN†

Abstract. We analyze three finite difference approximations of the nonlinear Klein–Gordon equation and show that they are directly related to symplectic mappings. Two of the schemes, the Perring–Skyrme and Ablowitz–Kruskal–Ladik, are long established, and the third is a new, higher order accurate scheme. We test the schemes on traveling wave and periodic breather problems over long time intervals and compare their accuracy and computational costs with those of symplectic and nonsymplectic method-of-lines approximations and a nonsymplectic energy conserving method.

Key words. symplectic approximations, Klein–Gordon equation, finite differences

AMS subject classifications. 65M99, 65M05, 65M20, 35Q20

PII. S0036142993243106

1. Introduction. The nonlinear Klein–Gordon equation,

$$(1) \quad u_{tt} - \Delta u + g(u) = 0,$$

is used to model many different nonlinear phenomena, including the propagation of dislocations in crystals and the behavior of elementary particles and of Josephson junctions (see [6, Chap. 8.2] for details). It has also been the subject of detailed investigation in studies of solitons and nonlinear science in general. It is probably best known as the sine-Gordon equation,

$$u_{tt} - \Delta u + \sin u = 0,$$

although it also appears with $g(u) = \sinh u$, polynomial $g(u)$, and other nonlinear functions. Details of existence, uniqueness, and other analytic properties of solutions of (1) can be found in [16], and a more general discussion, including applications and numerical approximations, can be found in [4] and [6]. We note that one key feature is that the Klein–Gordon equation is a Hamiltonian PDE, and for a wide class of functions $g(u)$ it has conserved Hamiltonian (or energy)

$$(2) \quad H = \int \left(\frac{1}{2} u_t^2 + \frac{1}{2} |\nabla u|^2 + G(u) \right) dx,$$

where $G'(u) = g(u)$.

Approximation of the Klein–Gordon equation by finite differences has long been used to investigate nonlinear phenomena such as the collision and interaction of solitary waves and other coherent structures and has mostly concentrated on work in one space dimension. The Perring–Skyrme (PS) approximation of the one-dimensional (1D) sine-Gordon equation, which is based on replacement of the second derivatives by second central differences, was introduced in [13] in 1962. Concerns with efficiency led to the introduction of the Ablowitz–Kruskal–Ladik (AKL) scheme [1], which is a

*Received by the editors January 19, 1993; accepted for publication (in revised form) January 2, 1996.

<http://www.siam.org/journals/sinum/34-5/24310.html>

†Department of Mathematics, Heriot-Watt University, Edinburgh, EH14 4AS, UK (d.b.duncan@ma.hw.ac.uk).

simple modification of the PS scheme and cuts the computation time in half without reducing the order of accuracy. Concerns with energy conservation also led to modifications, and schemes which exactly conserve a discrete approximation of the energy (2) are described and compared in [4, Chap. 10] and [9]. One popular scheme for studies in two dimensions is analogous to the AKL 1D scheme (see [4, Chap. 10]), and a new family of fourth-order accurate schemes for one dimension and two dimensions is derived and analyzed in [7]. We restrict our attention to 1D schemes for simplicity, since the issues we address are not dependent on the number of space dimensions.

Recently there has been a great deal of interest in numerical approximations of Hamiltonian systems of ODEs which share the symplectic (generalized area preservation) properties of the solution mapping of the ODEs. This is because symplectic schemes can produce better qualitative and quantitative results for Hamiltonian systems than standard ODE solvers, particularly when long time integrations are required. See [3, 10, 14, 15] and references therein, and also [12], which is written for a general scientific audience. This work is also relevant to the numerical approximation of Hamiltonian PDEs like the Klein–Gordon equation, which, when suitable space derivative approximations are used, is reduced to the approximate solution of a Hamiltonian system of ODEs in time (see [11] and [15]).

We discuss Hamiltonian PDEs below but first consider the system of Hamiltonian ODEs

$$\dot{\underline{p}} = -\nabla_q H(\underline{p}, \underline{q}), \quad \dot{\underline{q}} = \nabla_p H(\underline{p}, \underline{q}), \quad \underline{p}, \underline{q} \in \mathcal{R}^d,$$

where the dot denotes differentiation with respect to t , H is the Hamiltonian function, and the solution mapping $\psi_T : \mathcal{R}^{2d} \rightarrow \mathcal{R}^{2d}$ is defined by

$$\psi_T(\underline{p}(t_0), \underline{q}(t_0)) = (\underline{p}(t_0 + T), \underline{q}(t_0 + T)).$$

When $d = 1$, the mapping ψ_T is symplectic if it preserves area. That is, if $D \subset \mathcal{R}^2$ is a bounded subdomain in the domain of ψ_T , then the area of D is equal to the area of its image $\psi_T(D)$. In the general case $d \geq 1$, area is generalized to the sum of oriented areas of the surfaces D_i , which are the projections of D onto the (p_i, q_i) planes. Fortunately, this geometric condition can be checked relatively easily by the following result [15, Chap. 2.5].

DEFINITION 1. *A discrete mapping $\psi : \mathcal{R}^{2d} \rightarrow \mathcal{R}^{2d}$ is symplectic if*

$$(3) \quad D\psi^T J D\psi = J, \quad \text{where } J \equiv \begin{pmatrix} 0 & -I \\ I & 0 \end{pmatrix},$$

I is the d -dimensional identity matrix, and $D\psi$ is the Jacobian matrix of ψ .

Note that if $\underline{p}, \underline{q} \in \mathcal{R}^d$, then $\underline{p}^T J \underline{q}$ is the sum of oriented areas of the parallelograms determined by the projections of $\underline{p}, \underline{q}$ onto the (p_i, q_i) planes.

Moving from Hamiltonian ODEs to Hamiltonian PDEs, the symplectic mapping properties of the exact solution operator are generalized to Poisson mapping properties [11] and [15, Chap. 14], which again determine the dynamics of the solution. Properties of Poisson mappings can be exploited to design numerical approximations of Hamiltonian PDEs [11]. However, numerical approximations ultimately reduce to discrete mappings from time level to time level, and they reproduce Hamiltonian dynamics if they are symplectic. Thus we only require knowledge of the symplectic property of discrete maps to study the finite difference schemes we consider below, and so we do not discuss Poisson mappings further.

A systematic approach to obtaining a symplectic approximation of (1) is the method-of-lines, where the discretization is carried out in two distinct steps: the first is to approximate the space derivatives leaving a Hamiltonian system of ODEs in time (using second central difference approximations of the space derivatives, for example); the second is to solve the ODEs by an appropriate symplectic method. We only consider finite difference approximations of the space derivatives below, but the principle is the same when spectral and finite element methods are used in the space discretization. Examples of spectral symplectic method-of-lines approximations are given in [11]. The advantage of the method-of-lines approach (spectral or otherwise) is that off-the-shelf derivative approximations and ODE solvers can be used. The drawback is that to obtain overall high-order accuracy, both the space and time approximations must be high-order accurate, and wide difference stencils and multi-level ODE solvers are required. We describe fourth-order accurate method-of-lines schemes in section 2.

One of our main goals here is to show that certain standard finite difference approximations of (1) in space and time are directly related to symplectic mappings. This is despite being derived heuristically rather than systematically to preserve the Hamiltonian structure. In particular we show in section 3 that the PS scheme [13] is symplectic and that the widely used AKL scheme [1] is related to a symplectic map by a linear transformation. Both schemes were devised long before this became a consideration in numerical approximations. Also, in section 3, we show that the new fourth-order accurate finite difference scheme introduced in [7] is related to a symplectic map by a change of variables.

Another aim is to compare and assess the performance of the various schemes mentioned above, to see if the symplectic property does bring benefits to finite difference approximations of this PDE. In section 4 we present results from a series of test problems with traveling wave and time periodic pulsating “breather” solutions. We look at the qualitative behavior and the errors in symplectic and nonsymplectic schemes and make comparisons which take into account the computational effort as well as the results obtained.

The paper is organized in the following way. We continue in the next section with a brief description of various second- and fourth-order accurate finite difference and method-of-lines schemes for the Klein–Gordon equation. Then, in section 3 we show that three finite difference schemes discussed in section 2 are either symplectic or related to symplectic mappings by a transformation. We compare the performance of the various schemes in section 4 and finish with conclusions in section 5.

2. Finite difference schemes. In this section we briefly describe a collection of finite difference and method-of-lines approximations of the Klein–Gordon PDE (1) in one dimension. We refer to other sources for their derivation and for details of accuracy, stability, and convergence analyses.

We use the following notation throughout. The function $u(x, t)$ is approximated on a uniform space mesh with uniform time steps by $u_j^n \approx u(jh, n\tau)$, where h is the space mesh size and τ is the time step size. The ratio of time to space mesh size is $\lambda = \tau/h$ and is assumed to be $O(1)$ in h . Difference schemes are written in terms of the space and time second central difference operators δ_x^2, δ_t^2 defined by

$$(4) \quad \delta_x^2 u_j^n \equiv u_{j+1}^n - 2u_j^n + u_{j-1}^n, \quad \delta_t^2 u_j^n \equiv u_j^{n+1} - 2u_j^n + u_j^{n-1}$$

and are described as “explicit” if they can be advanced in time without the need to solve systems of algebraic equations. They are “implicit” otherwise.

2.1. Simple second-order scheme. A basic approximation of (1) in one dimension is obtained by replacing the derivatives by central differences to obtain

$$(5) \quad \delta_t^2 u_j^n - \lambda^2 \delta_x^2 u_j^n + \tau^2 g(u_j^n) = 0,$$

which is second-order accurate. This is the PS scheme introduced in [13]. It is a member of the general class

$$(6) \quad \delta_t^2 u_j^n - \tau^2 \Delta_h u_j^n + \tau^2 g(u_j^n) = 0,$$

where Δ_h is a difference approximation of the Laplacian operator. Such schemes are explicit and their implementation is straightforward. We show in section 3.2 that this class of schemes is symplectic.

2.2. Second order with spatial averaging. The original 1D PS scheme (5) is not stable with equal time and space mesh sizes and was modified in [1] to improve the stability and allow a unit mesh ratio $\lambda \equiv \tau/h = 1$ to be used. The term u_j^n in $g(u_j^n)$ is replaced by a local average of u over two neighboring space mesh points. After a little rearrangement, this modified scheme (known as the AKL scheme) can be written as

$$(7) \quad u_j^{n+1} = (2 - 2\lambda^2)u_j^n - u_j^{n-1} + 2\lambda^2 \bar{u}_j^n - \tau^2 g(\bar{u}_j^n),$$

where the local average \bar{u} is given by

$$\bar{u}_j^n = \frac{1}{2}(u_{j-1}^n + u_{j+1}^n).$$

This requires less computational effort than the simple 1D scheme (5) for two reasons. The first is that larger and hence fewer time steps can be used. The second reason is that when $\lambda = 1$, the term u_j^n vanishes and the approximate solution splits into two disjoint sets of odd and even numbered mesh points. Only one-half of the solution components are required at any time level, and thus a significant reduction in computer time is achieved.

A general form of this type of approximation, with or without the segregation of solution components into disjoint sets, is then

$$(8) \quad \delta_t^2 u_j^n - \tau^2 \Delta_h u_j^n + \tau^2 g(\alpha_h u_j^n) = 0,$$

where Δ_h is an approximation of the Laplacian operator and α_h is a spatial averaging operator. Schemes of this form are at most second-order accurate (to verify this, examine the accuracy of the ODE approximation obtained from (8) when u depends only on time t). Again, these schemes are explicit and can be implemented quite easily. We show in section 3.3 that this class of schemes is directly related to a symplectic mapping by a linear change of variables.

2.3. A second-order energy conserving scheme. Another variation of the standard second central difference approximation (5) given by Strauss and Vasquez in [17] is

$$(9) \quad \delta_t^2 u_j^n - \lambda^2 \delta_x^2 u_j^n + \tau^2 \left(\frac{G(u_j^{n+1}) - G(u_j^{n-1})}{u_j^{n+1} - u_j^{n-1}} \right) = 0,$$

where $G'(u) = g(u)$. This scheme is second-order accurate and implicit (it requires the solution of a scalar, nonlinear algebraic equation for u_j^n at each space point and time level). This scheme was designed to conserve a discrete approximation of the energy (2) given by

$$E_h^n = \frac{h}{2} \sum_j \left[\frac{(u_j^{n+1} - u_j^n)^2}{\tau^2} + \frac{(u_{j+1}^{n+1} - u_j^{n+1})(u_{j+1}^n - u_j^n)}{h^2} + G(u_j^{n+1}) + G(u_j^n) \right],$$

in the sense that $E_h^n = E_h^0$ for all $n \geq 0$.

This scheme is time reversible, but no change of variables has been found to relate it to a symplectic mapping, and it is believed to be unlikely that such a change of variable exists. This is discussed in [11] for the special case $g(u) = u^3$.

2.4. A fourth-order finite difference scheme. To achieve higher order accuracy it is necessary to use a more complicated difference scheme than those we have already described. The scheme we discuss here is the 1D version of a family of two-dimensional (2D) schemes derived and analyzed in [7] and based on linear wave equation schemes given in [8]. Efficient implementation of these schemes in more than one space dimension is addressed in [8], but these methods are not necessary for the 1D version discussed here.

We introduce the finite difference operator

$$M_h = 1 + \frac{1 - \lambda^2}{12} \delta_x^2$$

and then define the implicit difference scheme

$$(10) \quad M_h \delta_t^2 \left(u_j^n + \frac{\tau^2}{12} g_j^n \right) = \lambda^2 \delta_x^2 \left(u_j^n - \frac{\tau^2}{12} g_j^n \right) - \tau^2 M_h g_j^n,$$

which can be shown to be fourth-order accurate. The operator M_h is analogous to a finite element mass matrix. The implementation and analysis of the scheme is made easier when it is rewritten in the form

$$(11) \quad M_h \delta_t^2 \phi_j^n = \lambda^2 \delta_x^2 \phi_j^n - \tau^2 (M_h + \lambda^2 \delta_x^2 / 6) g(u(\phi_j^n)),$$

where the function $u(\phi)$ is defined implicitly by

$$(12) \quad \phi = u + \tau^2 g(u) / 12.$$

Scheme (11) is a member of the general class of implicit schemes

$$(13) \quad M_h \delta_t^2 \phi_j^n = \tau^2 L_h \phi_j^n - \tau^2 A_h g(u(\phi_j^n)),$$

where M_h and A_h are space averaging operators and L_h is a space differencing operator. To advance one step in time it is necessary to first solve a linear tridiagonal system of equations for the values ϕ_j^{n+1} (including boundary conditions) and then a scalar nonlinear equation (12) for each u_j^{n+1} in turn. We show in section 3.4 that this class of schemes is directly related to a symplectic mapping by a change of variables.

2.5. Fourth-order method-of-lines schemes. The method-of-lines approach to the approximation of (1) is composed of two stages: space and time discretization. First we approximate the space derivatives to obtain a semidiscrete scheme in the form

$$\ddot{u}_j = \Delta_h u_j - g(u_j),$$

where Δ_h is a difference approximation of the Laplacian operator. This second-order system of ODEs is rewritten in standard first-order form as

$$(14) \quad \dot{p}_j = \Delta_h q_j - g(q_j), \quad \dot{q}_j = p_j,$$

where $q \equiv u$ and $p \equiv u_t$. To obtain fourth-order accuracy overall, we use the fourth-order accurate Laplacian approximation

$$(15) \quad \Delta_h = h^{-2}(1 - \delta_x^2/12)\delta_x^2$$

coupled with a fourth-order ODE solver. The ODE system (14) is Hamiltonian when this space derivative approximation is used (see Lemma 1).

The special separable Hamiltonian form of the ODEs (14) allows the use of efficient Runge–Kutta–Nystrom and partitioned Runge–Kutta (PRK) methods of symplectic and nonsymplectic type (see [14, 15]). There are many different fourth-order accurate ODE solvers of these types, and we select one symplectic and one nonsymplectic solver which were designed to have an “optimal” local truncation error (see [15, Chap. 8.5.3] for details). These schemes performed well in the experiments reported in [15]. The symplectic solver was derived by Calvo and is described in [2, 15]. It can be implemented as a five-stage PRK method which requires four evaluations of function g and difference operator Δ_h for each time step after the first (which needs five). The nonsymplectic solver was derived by Dormand and Prince and is described in [5, 15]. It is a four-stage Runge–Kutta–Nystrom method which requires three evaluations of g and Δ_h for each step after the first (which needs four).

3. Symplectic properties of difference schemes. In this section we show that the PS scheme (5) is symplectic, the AKL scheme (7) is related to a symplectic mapping by linear transformation, and the fourth-order finite difference (FD4) scheme (11) is related to a symplectic mapping by a nonlinear transformation. In each case we relate the scheme (or a generalization of it) to a symplectic one-step approximation of a Hamiltonian system of ODEs.

Throughout this section we concentrate on finite-dimensional discretizations obtained when the PDE (1) is posed on a finite interval with energy conserving boundary conditions, e.g., periodic, $u = 0$, or $u_x = 0$. Note that the extension to the infinite-dimensional pure initial value problem case is relatively straightforward (see [10], for example), as is the extension from one to multiple space dimensions outlined in section 3.5. There is no need to extend the analysis to nonconserving boundary conditions, since then the solution mapping of the PDE is not symplectic and there is no reason to look for a symplectic approximation.

The main results below rely on symmetry and commutativity of certain matrices which contain the spatial finite difference operations used in the schemes. These restrictions are reasonable since difference operators on regular grids commute, and the operators commonly used to approximate this PDE have an even symmetry, making the matrices symmetric. (Indeed, one would intuitively expect the use of unsymmetric differences to destroy any nice properties a wave equation like (1) might have.)

Standard discretizations of the energy conserving boundary conditions preserve the symmetric structure and the commutativity of the matrices.

3.1. Basic results. We will show that each of the schemes studied in this section can be related to a standard, one-step approximation of a system of ODEs. The ODE system is defined in the next lemma, where it is shown to be Hamiltonian. The approximation of the ODEs is given in the second lemma and is shown to be a symplectic map. The dimension N which appears in the lemmas is the number of mesh points in the space domain, and the matrices B, C, E arise from the space difference operators used in the approximations.

LEMMA 1. *Let B, C, E be matrices $\in \mathcal{R}^{N \times N}$ and let the vector function $\underline{f}(\underline{x}) \in \mathcal{R}^N$ have j th component $f(x_j)$ for each $j = 1, \dots, N$, where the scalar function f is continuously differentiable. If the matrices B and E are symmetric, then the system of ODEs*

$$(16) \quad \begin{aligned} \underline{p}' &= B\underline{q} - C\underline{f}(C^T \underline{q}), \\ \underline{q}' &= E\underline{p} \end{aligned}$$

is Hamiltonian. The Hamiltonian function is

$$(17) \quad H(\underline{p}, \underline{q}) = \frac{1}{2} \underline{p}^T E \underline{p} - \frac{1}{2} \underline{q}^T B \underline{q} + \sum_{\beta=1}^N F(\{C^T \underline{q}\}_\beta),$$

where $F'(x) = f(x)$ and $\{\underline{x}\}_\beta$ is the β th component of vector \underline{x} .

Proof. The result can be verified by taking the gradient of the Hamiltonian function (17) with respect to \underline{p} and \underline{q} to obtain

$$\begin{aligned} \underline{p}' &= B\underline{q} - C\underline{f}(C^T \underline{q}) = -\nabla_{\underline{q}} H, \\ \underline{q}' &= E\underline{p} = \nabla_{\underline{p}} H, \end{aligned}$$

which is a standard form for a Hamiltonian system. See, for example, [15, Chap. 1] or standard texts on ODEs. \square

LEMMA 2. *If the system of ODEs (16) with $\underline{p}, \underline{q} \in \mathcal{R}^N$ satisfies the conditions of Lemma 1, then the approximation*

$$(18) \quad \begin{aligned} \underline{p}^{n+1} - \underline{p}^n &= \tau (B\underline{q}^n - C\underline{f}(C^T \underline{q}^n)), \\ \underline{q}^{n+1} - \underline{q}^n &= \tau E\underline{p}^{n+1}, \end{aligned}$$

where $(\underline{p}^n, \underline{q}^n)$ approximates $(\underline{p}(n\tau), \underline{q}(n\tau))$, is symplectic.

Proof. (See also [3, 10].) By assumption, the ODE system (16) is Hamiltonian. Also, the mapping from $(\underline{p}^n, \underline{q}^n)$ to $(\underline{p}^{n+1}, \underline{q}^{n+1})$ defined by (18) is symplectic since its Jacobian matrix

$$I + \tau \begin{pmatrix} 0 & B - C Df C^T \\ E & \tau E(B - C Df C^T) \end{pmatrix}$$

(where Df is the Jacobian matrix of \underline{f}) satisfies condition (3) of Definition 1. \square

3.2. Simple schemes. We start with difference schemes of the form (6), which include the simple PS central difference scheme. The PDE is posed on a finite space domain with energy conserving boundary conditions such as periodic or $u = 0$. Recall that the solution mapping is not expected to be symplectic if nonconserving boundary conditions are used. We rewrite the scheme in vector form as

$$(19) \quad \underline{u}^{n+1} - 2\underline{u}^n + \underline{u}^{n-1} = \tau^2 (L\underline{u}^n - \underline{g}(\underline{u}^n)),$$

where \underline{u} contains the space components u_j arranged in order, L is the matrix form of the difference operator Δ_h , and the vector function $\underline{g}(\underline{u})$ has β th component $g(u_\beta)$. We now show that this scheme is symplectic under relatively weak hypothesis.

THEOREM 1. *Difference schemes of the form (19) are symplectic with canonical variables \underline{u}' , \underline{u} and approximate a Hamiltonian ODE system with Hamiltonian function*

$$H(\underline{u}', \underline{u}) = \frac{1}{2} \underline{u}'^T \underline{u}' - \frac{1}{2} \underline{u}^T L \underline{u} + \sum_{\beta} G(u_{\beta}),$$

where $G'(u) = g(u)$, if the differentiation matrix L is symmetric and the scalar function g is continuously differentiable.

Proof. The approximation (19) and the ODE system it approximates can be rewritten in the canonical forms required by Lemmas 1 and 2, where the variables and matrices used in the lemmas are given by $\underline{p} = \underline{u}'$, $\underline{q} = \underline{u}$, $B = L$, $E = C = I$, and $g = f$. \square

The difference scheme (6) has a symmetric differentiation matrix L when even order central difference operators are used and standard approximations of the energy conserving boundary conditions are imposed. The theorem above implies that the scheme is symplectic when applied to the Klein–Gordon equation with a smooth enough nonlinear function $g(u)$.

3.3. Averaged schemes. It is not as easy to show that the averaged scheme (8) is related to a symplectic map. With the addition of suitable linear, homogeneous boundary conditions, it can be written as

$$(20) \quad \underline{u}^{n+1} - 2\underline{u}^n + \underline{u}^{n-1} = \tau^2 (L\underline{u}^n - \underline{g}(A\underline{u}^n)),$$

where L and A are the matrix versions of the Laplacian approximation and spatial averaging difference operators Δ_h and α_h . We note that the space difference operators in Δ_h and α_h commute, and if standard approximations of the energy conserving boundary conditions are used, the resulting matrices L and A also commute.

The main difficulty in proving that the scheme (20) is symplectic stems from the fact that the averaging matrix A can be singular (see Example 1 on the AKL scheme at the end of this section). We first state and prove a general theorem which works for both singular and nonsingular A , and then we give a simpler proof in the case when A is not singular.

THEOREM 2. *If the matrices L and A of (20) are symmetric and commute and g is continuously differentiable, then schemes of the form (20) are related by a linear transformation to a symplectic approximation of a Hamiltonian ODE with associated Hamiltonian*

$$H = \frac{1}{2} \underline{u}'^T A \underline{u}' - \frac{1}{2} \underline{u}^T A L \underline{u} + \sum_{\beta} G(\{A\underline{u}\}_{\beta}),$$

where $G' = g$ and $\{\underline{x}\}_{\beta} = x_{\beta}$ for vectors \underline{x} .

Proof. Note that the matrix A is not restricted to be nonsingular in this proof. Since A is real and symmetric it has an orthonormal basis of eigenvectors which we place in the columns of the matrix X . Note that $X^T X = I$. Since A and L commute and L is symmetric, L has the same eigenvectors as A [18, Chap. 1, sect. 50]. We can write $A = X D_A X^T$ and $L = X D_L X^T$, where D_A, D_L are real, diagonal matrices whose entries are the eigenvalues of A and L , respectively.

The next part of the proof is derived from [18, Chap. 4, sect. 43]. We define a diagonal matrix Z_A whose diagonal entries are ± 1 corresponding to the sign of the diagonal entries of the matrix D_A . We arbitrarily assign $+1$ to the element in Z_A corresponding to a 0 on the diagonal of D_A . We have $Z_A^2 = I$ and the matrix $|D_A| \equiv Z_A D_A$ is diagonal and positive semidefinite. We write $A = W Z_A W^T$, where $W \equiv X |D_A|^{1/2}$.

Now, multiplying the scheme (20) by $Z_A W^T$ and defining $\underline{q} = W^T \underline{u}$, we obtain

$$\begin{aligned} Z_A(\underline{q}^{n+1} - 2\underline{q}^n + \underline{q}^{n-1}) &= \tau^2 Z_A W^T L \underline{u}^n - \tau^2 Z_A W^T \underline{g}(W Z_A W^T \underline{u}^n) \\ &= \tau^2 Z_A D_L \underline{q}^n - \tau^2 Z_A W^T \underline{g}(W Z_A \underline{q}^n). \end{aligned}$$

This is rearranged (using $L = X D_L X^T$) as

$$\begin{aligned} \underline{p}^{n+1} - \underline{p}^n &= \tau Z_A D_L \underline{q}^n - \tau Z_A W^T \underline{g}(W Z_A \underline{q}^n), \\ (21) \quad \underline{q}^{n+1} - \underline{q}^n &= \tau Z_A \underline{p}^{n+1}, \end{aligned}$$

which has the form required for Lemma 2 and approximates the first-order system of ODEs

$$\begin{aligned} \underline{p}' &= Z_A D_L \underline{q} - Z_A W^T \underline{g}(W Z_A \underline{q}), \\ \underline{q}' &= Z_A \underline{p}. \end{aligned}$$

This is a Hamiltonian system, since it satisfies the conditions of Lemma 1 with $B = Z_A D_L$, $E = Z_A$, $C = W Z_A$, and Hamiltonian function

$$H = \frac{1}{2} \underline{p}^T Z_A \underline{p} - \frac{1}{2} \underline{q}^T Z_A D_L \underline{q} + \sum_{\beta} G(\{W Z_A \underline{q}\}_{\beta}).$$

Thus, scheme (21) is symplectic. Using the relationship $\underline{q} = W^T \underline{u}$ and $\underline{p} = Z_A W^T \underline{u}'$ between the original variables \underline{u} and the canonical variables, we obtain the desired result. \square

Note that the matrix W used in the theorem above can be singular and that there may be other ways to relate the original scheme to a symplectic mapping. Indeed, we see below that when A is nonsingular, a much simpler proof of Theorem 2 is possible, and it involves a different symplectic mapping.

Remark. Assume that A is nonsingular in addition to the conditions of Theorem 2. We multiply the scheme (20) by A to obtain

$$A(\underline{u}^{n+1} - 2\underline{u}^n + \underline{u}^{n-1}) = \tau^2 A L \underline{u}^n - \tau^2 A \underline{g}(A \underline{u}^n),$$

which we rewrite as

$$\begin{aligned} \underline{p}^{n+1} - \underline{p}^n &= \tau A L \underline{q}^n - \tau A \underline{g}(A \underline{q}^n), \\ \underline{q}^{n+1} - \underline{q}^n &= \tau A^{-1} \underline{p}^{n+1}, \end{aligned}$$

where we define $\underline{q} = \underline{u}$. This is our standard approximation of the ODE system

$$\begin{aligned} \underline{p}' &= AL\underline{q} - A\underline{g}(A\underline{q}), \\ \underline{q}' &= A^{-1}\underline{p} \end{aligned}$$

with canonical variables $\underline{q} = \underline{u}$ and $\underline{p} = A\underline{u}'$. The system of ODEs is Hamiltonian using Lemma 1 since AL and A^{-1} are symmetric and the other conditions are also satisfied. Thus, the conditions of Lemmas 1 and 2 are satisfied and the scheme is symplectic. The form of the Hamiltonian also follows from Lemma 1.

Now we examine the AKL scheme in detail.

Example 1. The 1D scheme (7) with periodic boundary conditions has the form (20), and the matrices L and A have nonzero elements

$$l_{j,j-1} = 1/h^2, \quad l_{j,j} = -2/h^2, \quad l_{j,j+1} = 1/h^2,$$

and

$$a_{j,j-1} = \frac{1}{2}, \quad a_{j,j+1} = \frac{1}{2}$$

for $j = 1, \dots, N$ with $j \pm 1$ taken modulo N to accommodate the periodic boundary conditions. The matrices L and A are symmetric and commute, and A has eigenvalues

$$\Lambda(A)_j = \cos(2j\pi/N)$$

for $j = 1, \dots, N$. The matrix A is singular when N is even and nonsingular when N is odd. The right eigenvector \underline{x}^j associated with eigenvalue $\Lambda(A)_j$ has k th element

$$x_k^j = \cos(2jk\pi/N)$$

for $k = 1, \dots, N$. This is also an eigenvector of L .

Hence, if g is sufficiently smooth, the AKL scheme satisfies the conditions of Theorem 2 and is thus directly related to a symplectic mapping.

3.4. Implicit schemes. Now we examine fully implicit schemes like (13), which include the fourth-order accurate method (11). We assume that τ , $g(u)$, and u are restricted so that we can find u as a single-valued function of ϕ from the relationship

$$\phi = u + \tau^2 g(u)/12$$

and define $\gamma(\phi) \equiv g(u(\phi))$. Again, imposing suitable boundary conditions, we write the implicit scheme (13) in vector form as

$$(22) \quad M(\underline{\phi}^{n+1} - 2\underline{\phi}^n + \underline{\phi}^{n-1}) = \tau^2 (L\underline{\phi}^n - A\underline{\gamma}(\underline{\phi}^n)),$$

where A, L, M are the matrix versions of the difference operators A_h, L_h, M_h (including boundary conditions). We note again that the matrices A, L, M in the scheme are obtained from symmetric space difference operators and discretizations of the energy conserving boundary conditions, and so they all commute as required.

THEOREM 3. *If γ is continuously differentiable and if the matrices $A, L,$ and M are symmetric and commute and A and M are nonsingular, then schemes having the form (22) are symplectic approximations of a Hamiltonian ODE with canonical variables $\underline{p} = A^{-1}M\underline{\phi}'$ and $\underline{q} = \underline{\phi}$ and Hamiltonian*

$$H = \frac{1}{2}\underline{\phi}'^T A^{-1}M\underline{\phi}' - \frac{1}{2}\underline{\phi}^T A^{-1}L\underline{\phi} + \sum_{\beta} \Gamma(\phi_{\beta}),$$

where $\Gamma' = \gamma$.

Proof. We multiply the scheme (22) by A^{-1} to obtain

$$A^{-1}M(\underline{\phi}^{n+1} - 2\underline{\phi}^n + \underline{\phi}^{n-1}) = \tau^2 A^{-1}L\underline{\phi}^n - \tau^2 \underline{\gamma}(\underline{\phi}^n),$$

which we can rewrite as

$$\begin{aligned} \underline{p}^{n+1} - \underline{p}^n &= \tau A^{-1}L\underline{q}^n - \tau \underline{\gamma}(\underline{q}^n), \\ \underline{q}^{n+1} - \underline{q}^n &= \tau M^{-1}A\underline{p}^{n+1}, \end{aligned}$$

where we define $\underline{q} = \underline{\phi}$. This is the standard approximation of the ODE system

$$\begin{aligned} \underline{p}' &= A^{-1}L\underline{q} - \underline{\gamma}(\underline{q}), \\ \underline{q}' &= M^{-1}A\underline{p} \end{aligned}$$

with canonical variables \underline{q} and $\underline{p} = A^{-1}M\underline{\phi}'$. Lemma 1 implies that the system of ODEs is Hamiltonian, since $A^{-1}L$ and $M^{-1}A$ are symmetric (A, L, M commute and are symmetric) and the other conditions are also satisfied. Thus, the conditions of Lemma 2 are satisfied and the scheme is symplectic. The form of the Hamiltonian also follows from Lemma 2. \square

The proof relies on A and M being nonsingular. It is reasonable to expect M to be nonsingular since otherwise the difference scheme (13) cannot be advanced in time and would not be of any practical use. The restriction that A be nonsingular can be relaxed, and the proof becomes more complicated and similar to that of Theorem 2.

Example 2. The 1D scheme (11) with periodic boundary conditions has the form (22), where the matrices A, L, M are real and symmetric and have the same eigenvectors \underline{x}^j ($j = 1, \dots, N$) with elements

$$x_k^j = \cos(2jk\pi/N)$$

for $k = 1, \dots, N$. Thus, A, L, M commute with one another and A, M have eigenvalues

$$\Lambda(A)_j = 2/3 - \lambda^2/3 \sin^2(j\pi/N) \quad , \quad \Lambda(M)_j = 2/3 + \lambda^2/3 \sin^2(j\pi/N)$$

for $j = 1, \dots, N$. Matrix M is nonsingular for all mesh ratios λ , and A is certainly nonsingular when $\lambda \leq 1$, which is necessary for linear stability of the scheme.

The function $\underline{\gamma}(\underline{\phi}) \equiv g(u(\underline{\phi}))$ is defined implicitly by (12), and we assume that the time step size τ and nonlinear term $g(u)$ are such that (12) gives a one-to-one relationship between u and ϕ . We also require $\underline{\gamma}(\underline{\phi})$ to be continuously differentiable. All these conditions are guaranteed if g is continuously differentiable and

$$1 + \tau^2 g'(u)/12 > 0$$

for all u . This is certainly possible if $g'(u) \geq -c^2 > -\infty$ for some real constant c , which is true for many of the standard Klein-Gordon equations (e.g., $g(u) = \sin u, \sinh u, u^3 - u$).

Thus, for suitable functions $g(u)$ and small enough time step size, the scheme (11) is directly related to a symplectic map by a change of variables.

3.5. Extension to higher dimensions. The results of the previous sections can easily be extended to analogous difference schemes in two or more space dimensions since they have essentially the same form as the 1D schemes (19), (20), (22). The matrices that appear still have the required properties, since the multidimensional difference operations they are generated from commute and are symmetric.

TABLE 1

Summary of the schemes from section 2 tested in this section. Under “Type,” FD means finite difference and MOL means method-of-lines. Under “Map,” S means symplectic, TS means transformed symplectic, and NS means not symplectic.

Label	Type	Map	Order	Description
PS	FD	S	2	PS scheme (5)
AKL	FD	TS	2	AKL scheme (7)
SV	FD	NS	2	Strauss–Vasquez (SV) energy conserving scheme (9)
FD4	FD	TS	4	Implicit scheme (11)
C	MOL	S	4	Calvo (C) ODE solver with (15)
DP	MOL	NS	4	Dormand–Prince (DP) ODE solver with (15)

4. Results. In this section we report the results of applying the various methods described above to test problems. The schemes and some of their properties are listed in Table 1.

When measuring the error in an approximate solution at a given time level, we include contributions from the solution u and its time derivative u_t to see how the approximate solutions behave in the full phase space of the problem. However, similar results are obtained by examining the u components alone. The method-of-lines schemes compute direct approximations of u and u_t at each time step, but the finite difference schemes only approximate u directly. To measure the error contribution from the u_t terms in the finite difference schemes, we compare the “exact” and approximate central difference approximations

$$(u(x, t + \tau) - u(x, t - \tau))/2\tau \quad \text{and} \quad (u_j^{n+1} - u_j^{n-1})/2\tau$$

of $u_t(x, t)$. We define the discrete norm $\|\cdot\|_{1,h}$ of the function $f(x, t)$ by

$$\|f(\cdot, t)\|_{1,h}^2 = h \sum_j f(jh, t)^2 + \partial_t f(jh, t)^2$$

(with an analogous definition for mesh functions), where ∂_t represents the time derivative when dealing with the method-of-lines schemes and the second-order central difference approximation of the time derivative in the finite difference cases.

4.1. Stationary breather. The first set of results is for a breather solution of the sine-Gordon equation

$$u_{tt} - u_{xx} + \sin u = 0$$

given by

$$(23) \quad u(x, t) = 4 \tan^{-1} \left(\frac{\sqrt{1 - \omega^2}}{\omega} \frac{\cos \omega t}{\cosh(x\sqrt{1 - \omega^2})} \right)$$

for $w^2 < 1$ and $x \in \mathcal{R}$. This is a bump-shaped solution with peak value at $x = 0$ which oscillates up and down with period $2\pi/\omega$. The size of the solution decays exponentially away from the peak, and the infinite space domain for this problem can be truncated without significant effect on the approximate solutions obtained. We use domain $-L/2 \leq x \leq L/2$ with periodic boundary conditions and test with various choices of L to ensure that L is big enough to make the truncation effects negligible.

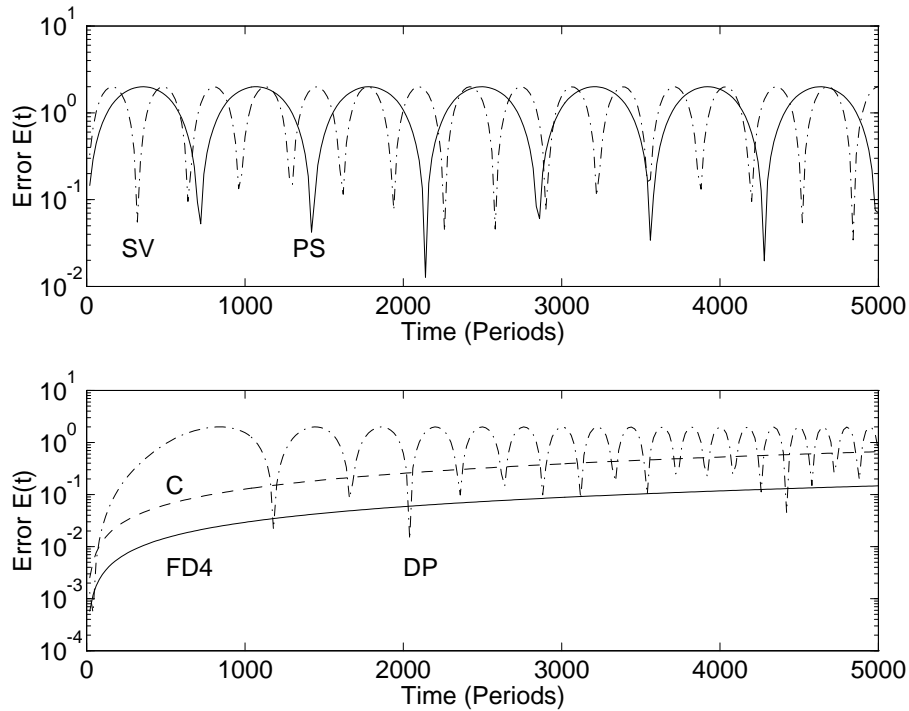


FIG. 1. Error $E(t)$ vs. time (measured every 10 periods) for the stationary breather test problem with $N = 512$, $L = 120$, and $\omega = 0.9$. The upper plot shows results from the second-order accurate schemes and the lower shows the fourth-order schemes.

The results described below were obtained with $N = 512$, $L = 120$, and $\omega = 0.9$. The AKL scheme only runs with mesh ratio $\lambda = 1$; all the other schemes were run with $\lambda = 0.5$ to satisfy stability restrictions and for easy compatibility with the AKL step sizes. The width of the breather at half its height covers about 27 mesh intervals. We chose the parameters so that the period of the breather oscillation, $2\pi/\omega$, is equal to an integer number of time steps.

In Figure 1 we show a graph of the relative error,

$$E(t) = \|u^n - u(\cdot, n\tau)\|_{1,h} / \|u(\cdot, n\tau)\|_{1,h}$$

(measured every 10 periods) against time for most of the schemes listed in Table 1 and see that the PS, Strauss–Vasquez (SV), and Dormand–Prince (DP) scheme errors are oscillatory. We omit the AKL results, which are similar to those of the PS scheme but with faster oscillations. Closer inspection reveals that the PS and SV schemes seem to have a regular period and the DP scheme oscillations get faster. On this graph, the FD4 and Calvo (C) errors increase monotonically, but this is just part of the first cycle in a regular series of very slow oscillations. All the schemes have a peak error of about 2. Snapshots of the approximate solutions (not shown here) show coherent, bump-shaped features oscillating regularly at a slightly different period than the exact solution. This difference is smaller for the more accurate schemes FD4 and C. The error maxima occur when the approximations are out of phase with the exact solution, and the minima occur when they are in phase.

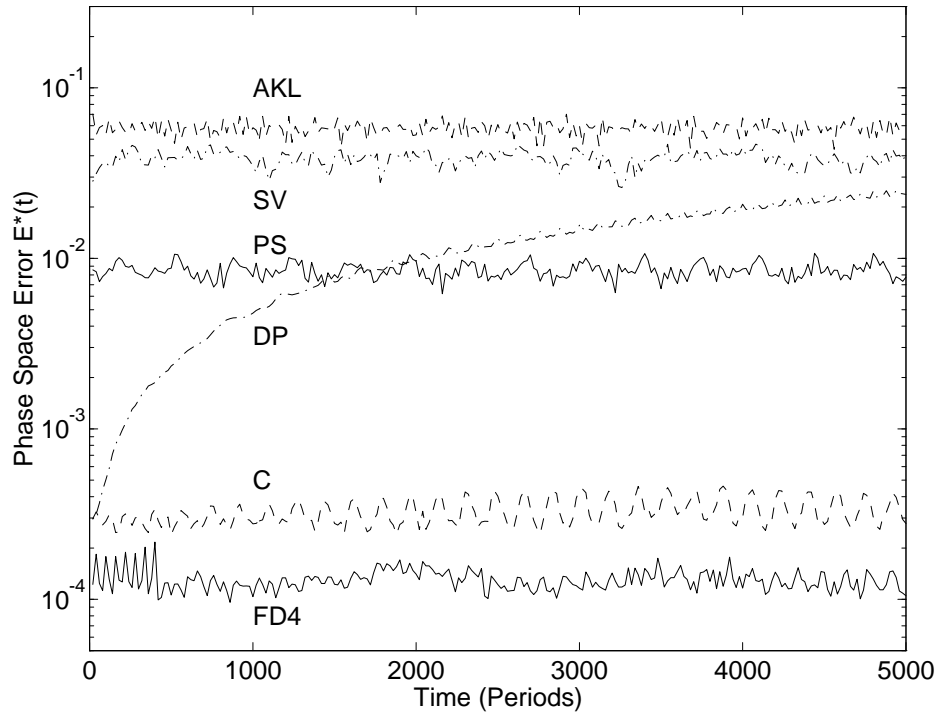


FIG. 2. Phase space error $E^*(t)$ vs. time (measured every 10 periods) for the problem in the previous figure. The two nonsymplectic schemes are SV and DP.

To investigate this further, we measure how far the approximate solution at time $n\tau$ is from the periodic orbit traced out by the exact solution in the $2N$ -dimensional phase space $\{(u(jh, t), u_t(jh, t)), j = -N/2, \dots, N/2 - 1\}$. We measure this distance in the norm $\|\cdot\|_{1,h}$ introduced above and normalize it by the size of the exact solution, giving the quantity

$$E^*(n\tau) = \min_{\eta} \|u^n - u(\cdot, \eta)\|_{1,h} / \|u(\cdot, \eta)\|_{1,h} .$$

We plot $E^*(t)$ against time in Figure 2 and see that only the nonsymplectic DP scheme drifts away from the exact solution orbit over very long time periods.

4.2. Traveling wave. We also test the schemes on traveling waves in the Phi-4 equation,

$$u_{tt} - u_{xx} + u^3 - u = 0 ,$$

which is described in [4]. The Phi-4 equation has traveling wave solutions,

$$(24) \quad u(x, t) = \pm \tanh \left((x - vt) / \sqrt{2(1 - v^2)} \right)$$

for $x \in \mathcal{R}$, with the velocity restricted by $v^2 < 1$. This traveling wave is a kink; that is, it consists of a single transition region between the asymptotic values $u = \pm 1$ as $x - vt$ varies between $\pm\infty$. Again this solution is on the whole real line, and again it quickly approaches its asymptotic values away from the transition region.

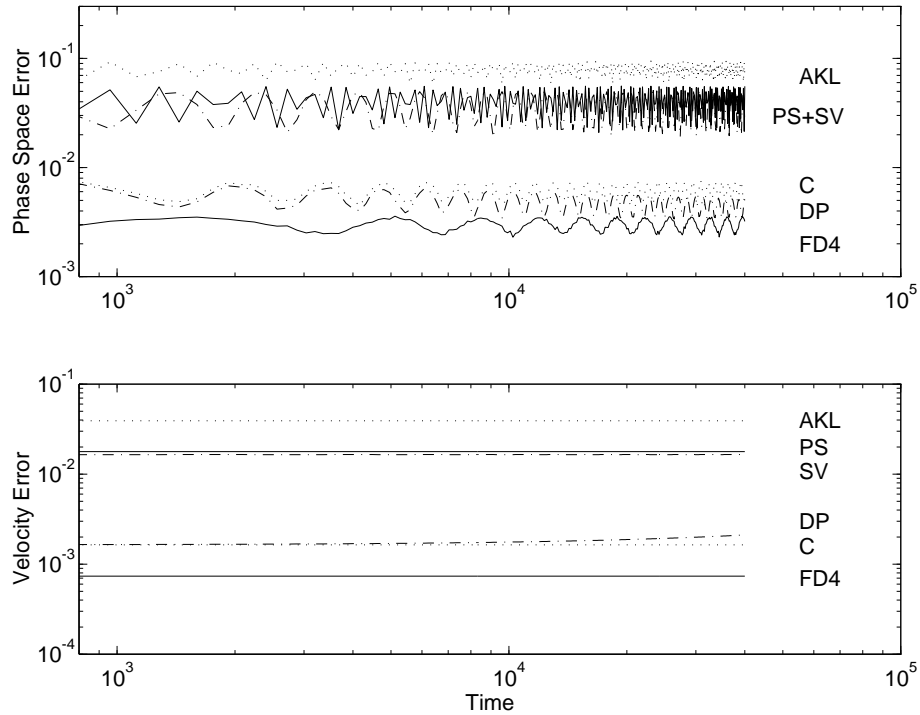


FIG. 3. Phase space error $E^*(t)$ and the relative error in the wave velocity plotted against time (measured every 40 units) for the traveling wave test with $N = 1024$, $L = 512$, $v = 0.5$. The approximate solutions are slower than the exact.

To reduce the problem to a finite computational domain, we consider the pure initial value problem with L -periodic initial data consisting of an alternating sequence of $+\tanh$, $-\tanh$ kinks spaced distance $L/2$ apart, each with the same value of v . Thus, we need only consider the domain $x \in [0, L]$ with periodic boundary conditions. When L is big enough, the kinks are far enough apart for their influence on one another to be negligible, and they propagate undistorted with velocity v . We try various values of L in the numerical tests to make sure that it is big enough.

The results described here were obtained with $N = 1024$, $L = 512$, and $v = 0.5$. The mesh ratio was $\tau/h = 0.5$ for all cases except the AKL scheme, which is again run with mesh ratio $\tau/h = 1$. The transition region from $u = -0.999$ to $u = +0.999$ covers about 19 mesh intervals. In contrast to the previous example, the error $E(n\tau) = \|u^n - u(\cdot, n\tau)\|_{1,h}$ in each scheme grows essentially monotonically with time. More importantly, we see in Figure 3 that the absolute error in phase space,

$$E^*(n\tau) = \min_{\eta} \|u^n - u(\cdot, \eta)\|_{1,h}$$

(with minimum value at $\eta = \eta^*$), does not grow perceptibly with time. We also extract information about the speed of the approximate wave by comparing η^* with the time t and find that each of the approximate solutions travels slightly too slowly but with nearly constant speed after a short settling-in period. Thus, the approximate solutions propagate nearly undistorted at a constant but slightly wrong speed, and the transition regions in the approximate and exact solutions get increasingly out of step, causing the observed monotonic increase in the error $E(t)$.

TABLE 2

Computer time per time step for the various schemes relative to the PS time, all measured on a Sun Sparc ELC computer. Results are averaged over a wide range of mesh sizes and over a large number of time steps.

Test	PS	AKL	SV	FD4	DP	C
Breather	1	0.57	10.8	6.5	5.4	6.6
Traveling wave	1	0.56	5.5	7.6	8.0	9.4

Also, in Figure 3 we see a hint that the nonsymplectic DP scheme is behaving differently from the others since its velocity changes marginally. In fact, the DP traveling wave slows down slightly. However, after much longer tests comparing the symplectic C and nonsymplectic DP schemes, very little difference could be detected in the quality of their solutions.

4.3. Efficiency. To measure the efficiency of the schemes in Table 1, we rerun the breather and traveling wave tests described above over a range of different mesh sizes and record the computer time required (on a 33MHz Sun Sparcstation ELC), as well as the real and phase space errors. The most efficient scheme is the one that produces a solution of a given accuracy with the least computational effort.

As a crude measure of the computational effort per time step in each of the schemes, we compare the time taken per step, relative to the time taken by the PS scheme and averaged over many different mesh sizes and a large number of time steps. Table 2 shows a summary of the results. In it we see that as expected the AKL scheme requires about half the effort of the PS, since only half the space points are updated at each time level. The largest variation in results between the two tests is probably due to the difference in the time taken in the evaluation of the nonlinear function $g(u)$. This is lower in the traveling wave test, and so the difference operations and auxiliary calculations are more significant there. The SV and FD4 schemes involve solving nonlinear algebraic equations at each point in space and time, and the effort required for this depends on the problem and the behavior of the solution. Typically, fewer iterations are required where the solution changes slowly.

In Figure 4 we plot the real error, the phase space error, and the relative error in the velocity of the wave against computer time for the traveling wave test with $v = 0.5$ and $L = 512$. We see that the second- and fourth-order accuracy of the schemes shows clearly in the different slopes of their graphs. Since the phase space and velocity errors do not change significantly over long times, their graphs can be taken as representative of the performance of the schemes over all but the shortest time periods. For comparison, we also show the error against mesh size and note that the second- and fourth-order convergence of the schemes shows very clearly. Figure 4 also shows that the fourth-order accurate schemes are more efficient than the second-order schemes when all but the crudest mesh resolution is used. The AKL scheme is generally the best of the second-order schemes, and the energy conserving SV scheme is the worst. This is because the AKL scheme is taking half as many time steps and updating half as many solution components as the others, and the SV scheme involves the solution of nonlinear equations at each space point and time level. Of the fourth-order schemes, FD4 is more efficient than the two method-of-lines schemes, which perform roughly equally well in this test.

5. Conclusions. Section 2 consists of a collection of finite difference and finite difference method-of-lines schemes for the approximate solution of the nonlinear

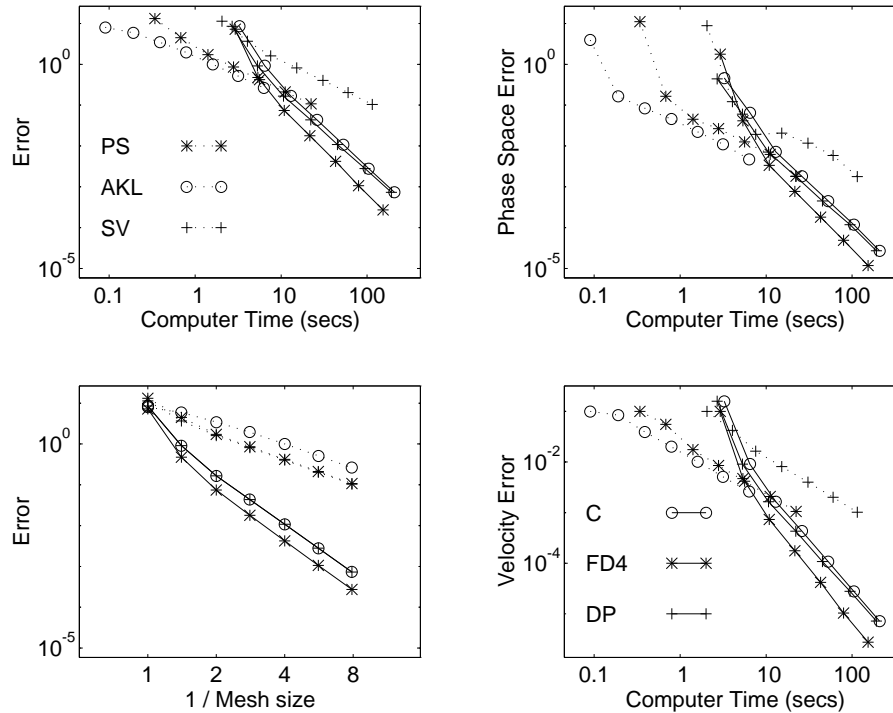


FIG. 4. Errors measured at $t = 128$ plotted against computer time and mesh size for the traveling wave test with $L = 512$, $v = 0.5$ and mesh sizes from $1/8$ to 1 . We use solid and dotted lines for the fourth- and second-order schemes, respectively.

Klein–Gordon equation in one space dimension. Some of these schemes have been known and used for many years, but the high-order accurate finite difference scheme (11) is more recent, and the method-of-lines schemes do not appear to have been investigated before. In section 3 it is shown that the long-used PS scheme is symplectic and that the AKL and FD4 schemes are directly related to symplectic mappings by a change of variables. In a sense, it is hard to avoid producing schemes related to symplectic mappings if central difference operators in space and time are used to approximate the Klein–Gordon equation. However, the energy conserving scheme (9) spoils this simple generalization, since it is believed to not be related to a symplectic mapping.

Section 4 contains test results for the various schemes on periodic breather and traveling wave test problems. In the traveling wave tests, it is found that all the schemes produce waves with little change in shape and speed over long time intervals. The main error in the results is due to the wave speed being slightly wrong. In the time periodic breather test, all apart from the nonsymplectic DP method-of-lines scheme produce a solution which maintains its shape and a nearly constant (but slightly wrong) period of oscillation for very long times, and the DP scheme produces an oscillating solution which gradually decays in amplitude and speeds up. The failure of the DP scheme in the breather test is due to its dissipative nature, and the success of the other nonsymplectic scheme (the energy conserving SV scheme (9)) is probably due to the fact that it is time reversible and also captures some qualitative features of Hamiltonian dynamics (see [11]).

Assessments of the efficiency of the schemes show that the energy conserving scheme is least efficient (due to its low order of accuracy and the need to solve nonlinear algebraic equations at each time level) and the FD4 scheme (11) is most efficient (despite having to solve nonlinear algebraic equations at each time level). The FD4 scheme is derived by an optimal combination of second-order space and time discretizations to give fourth-order accuracy overall, and the method-of-lines schemes involve independent fourth-order accurate approximations in space and time, which are more complicated and hence involve more computational effort. The results suggest that if high-accuracy solutions are not required, then the PS or AKL scheme should be used (PS is probably easier to code), and the fourth-order scheme (11) should be used for high accuracy.

Finally, we note that the proofs relating finite difference schemes to symplectic mappings can be applied directly to schemes in more than one space dimension. Preliminary experiments with multidimensional schemes analogous to the 1D methods above produce broadly similar results. Indeed, these experiments indicate that the FD4 scheme looks even more efficient than the method-of-lines schemes in higher dimensions, where the wide stencil of the method-of-lines Laplacian approximation becomes more significant.

Acknowledgments. The author would like to thank K. J. Brown, P. J. Davies, and J. C. Eilbeck for help and encouragement in the preparation of this paper, and the referee for useful suggestions. The computing equipment was provided by the UK SERC Nonlinear Systems Initiative.

REFERENCES

- [1] M. J. ABLOWITZ, M. D. KRUSKAL, AND J. F. LADIK, *Solitary wave collisions*, SIAM J. Appl. Math., 36 (1979), pp. 428–437.
- [2] M. P. CALVO AND J. M. SANZ-SERNA, *High order symplectic Runge–Kutta–Nystrom methods*, BIT, 32 (1992), pp. 131–142.
- [3] P. J. CHANNELL AND C. SCOVEL, *Symplectic integration of Hamiltonian systems*, Nonlinearity, 3 (1990), pp. 231–259.
- [4] R. K. DODD, J. C. EILBECK, J. D. GIBBON, AND H. C. MORRIS, *Solitons and Nonlinear Wave Equations*, Academic Press, New York, 1982.
- [5] J. R. DORMAND, M. E. A. EL-KIKKAWY, AND P. J. PRINCE, *Families of Runge–Kutta–Nystrom formulae*, IMA J. Numer. Anal., 7 (1987), pp. 235–250.
- [6] P. J. DRAZIN AND R. S. JOHNSON, *Solitons: An Introduction*, Cambridge University Press, Cambridge, UK, 1989.
- [7] D. B. DUNCAN, *High Order Accurate and Isotropic Approximations of the Nonlinear Klein–Gordon Equation*, preprint, 1994.
- [8] D. B. DUNCAN AND M. A. M. LYNCH, *Jacobi iteration in implicit approximations of the wave equation*, SIAM J. Numer. Anal., 28 (1991), pp. 1661–1679.
- [9] S. JIMENEZ AND L. VAZQUEZ, *Analysis of four numerical schemes for a nonlinear Klein–Gordon equation*, Appl. Math. Comput., 35 (1990), pp. 61–94.
- [10] F. KANG AND Q. MENG-ZHAO, *The symplectic methods for the computation of Hamiltonian equations*, in Numerical Methods for Partial Differential Equations, Zhu You-Lan and Guo Ben-Yu, eds., Lecture Notes in Mathematics 1297, Springer-Verlag, Berlin, 1987, pp. 1–37.
- [11] R. MCLACHLAN, *Symplectic integration of Hamiltonian wave equations*, Numer. Math., 66 (1994), pp. 465–492.
- [12] R. MCLACHLAN, *The world of symplectic space*, New Scientist, 141 (1994), pp. 32–35.
- [13] J. K. PERRING AND T. H. R. SKYRME, *A model unified field equation*, Nuclear Phys., 31 (1962), pp. 550–555.
- [14] J. M. SANZ-SERNA, *Symplectic integrators for Hamiltonian problems: An overview*, in Acta Numerica 1992, A. Iserles, ed., Cambridge University Press, Cambridge, UK, 1992, pp. 243–286.

- [15] J. M. SANZ-SERNA AND M. P. CALVO, *Numerical Hamiltonian Problems*, Chapman and Hall, London, 1994.
- [16] W. A. STRAUSS, *Nonlinear Wave Equations*, Regional Conference Series in Mathematics, Vol. 73, AMS, Providence, RI, 1989.
- [17] W. A. STRAUSS AND L. VAZQUEZ, *Numerical solution of a nonlinear Klein-Gordon equation*, J. Comp. Phys., 28 (1978), pp. 271–278.
- [18] J. H. WILKINSON, *The Algebraic Eigenvalue Problem*, Oxford University Press, Oxford, UK, 1965.